

# Trends in Tropical Wave Activity from the 1980s to 2016

Ajay Raghavendra, Paul E. Roundy, and Liming Zhou

Email: araghavendra@albany.edu | 2019 American Meteorological Society Annual Meeting, Phoenix, AZ



## Background and Motivation

- Convectively coupled Atmospheric equatorial waves are strongly linked to the dynamics observed in the Earth's atmosphere. These waves may help us better understand atmospheric convection, precipitation characteristics, and energy redistribution.
- From the standpoint of climate change and variability, understanding tropical wave dynamics and interactions may help us better project cloud and rainfall distribution both in the present and possible future climate scenarios.
- GCMs (e.g., CMIP5 models) struggle to produce realistic tropical wave activity e.g., the MJO (Hung et al. 2013, *J. Climate*).

## $T_b$ and OLR Data from 15°N–15°S

- Geostationary Satellites: Gridded infrared (IR) channel brightness temperature ( $T_b$ ) dataset (GridSat-B1; Knapp 2008, *BAMS*) → Data procured from 1982–2016 (35 years) at 0.07-degree latitude equal-angle grid at a 3-hour temporal resolution → Re-gridded to 0.98-degree grid and 24-hour temporal resolution to speed-up calculations and for easy comparison with the OLR dataset
- Polar Orbiting Satellites: Interpolated OLR dataset (Liebmann and Smith 1996, *BAMS*) by NOAA from 1979–2016 (38 years) with a temporal resolution of 1-day, a horizontal resolution of 2.5°×2.5°

## Method

- Remove the seasonal cycle in both datasets using five pairs of harmonics to the annual cycle (Roundy 2017, *QJRM*).
- Wheeler and Kaladis (1999, *JAS*) Frequency–Wavenumber Power Spectrum
- Compute the symmetric and antisymmetric parts of the datasets:
 
$$Y_{\text{symm}} = \frac{Y_{\text{anom}}(15^{\circ}\text{N}-0^{\circ}) + Y_{\text{anom}}(15^{\circ}\text{S}-0^{\circ})}{2}$$

$$Y_{\text{asym}} = \frac{Y_{\text{anom}}(15^{\circ}\text{N}-0^{\circ}) - Y_{\text{anom}}(15^{\circ}\text{S}-0^{\circ})}{2}$$
- 200-day segmentation time window repeated every 100-day. Detrend and apply a Cosine bell each time window.
- Apply a discrete Fourier transform (DFT) for each 200-day time window iteratively to obtain  $FFT(Y_{\text{symm}})$  and  $FFT(Y_{\text{asym}})$ .
- Calculate symmetric and antisymmetric power by taking the complex conjugate.

## Results (Part 1: Trends in Spectral Power)

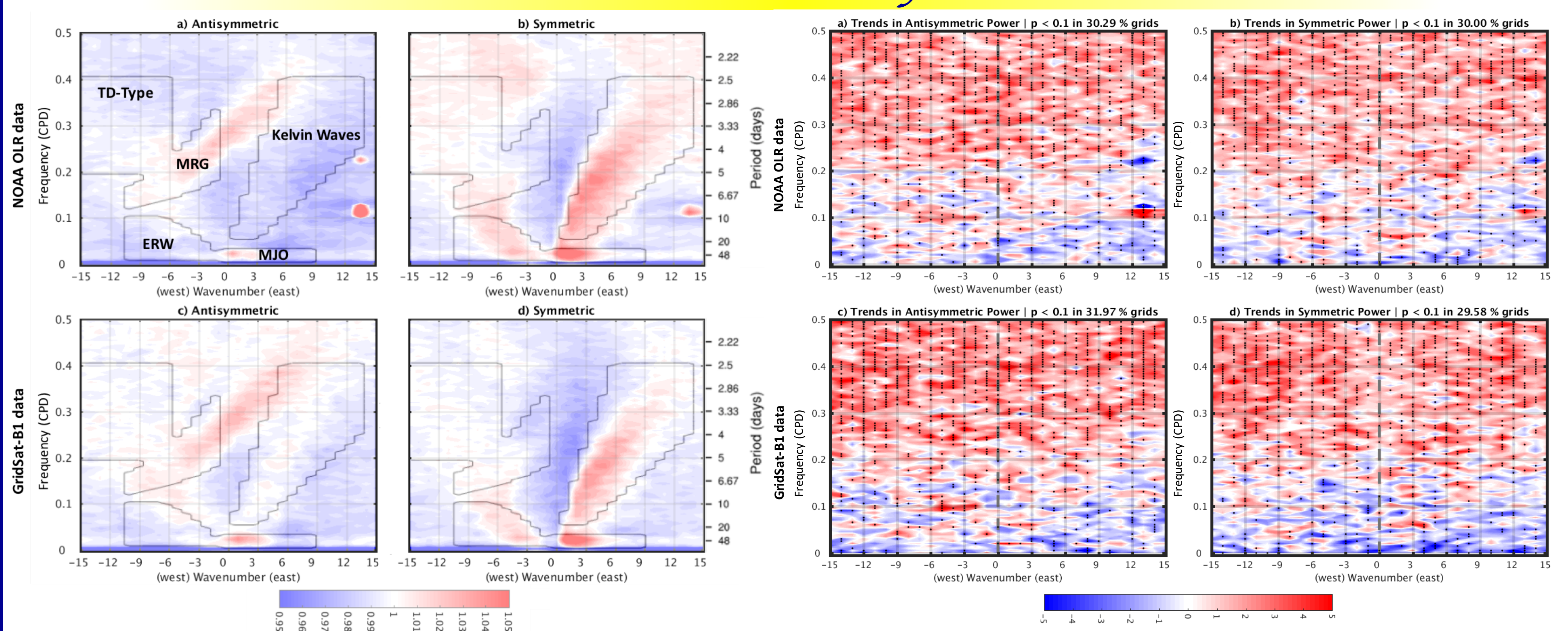


**Fig 1:** The frequency-wavenumber power spectrum diagram normalized by the smoothed background spectrum similar to the technique developed by WK99.

**Fig 2:** Linear trends in the  $\log_e$  spectral power ( $\times 10^{-3}$ ) from 1979–2016 for the OLR dataset and 1982–2016 for the  $T_b$  dataset. The black dots indicate trends that are statistically significant ( $p$ -value<0.1).

## Summary

- Good agreement** in the mean power spectrum and trends between the  $T_b$  and OLR datasets:
  - Significant decrease in  $P$  from  $\sim 0-0.2$  cpd, and an increase in  $P$  from  $\sim 0.2-0.5$  cpd.
  - Over 30% of the power spectrum diagram shows significant trends ( $p$ -value<0.1)
- Increase in power at high  $f$**  (e.g., KWs, MRG, and TD-type) coincides with a significant increase in the occurrence of high frequency disturbances, accompanied by a decrease the mean duration of an event.
- Decrease in power at low  $f$**  (e.g., MJO and ERW) is associated with spatially non-homogeneous trends in the mean duration and number of the events. These changes appear to trend towards producing spatially homogeneous MJO characteristics.
- Trends in spatial variance and power agree well with each other i.e., increase in power corresponds to an increase in variance.

## Results (Part 2: Trends in Tropical Waves and Confidence)

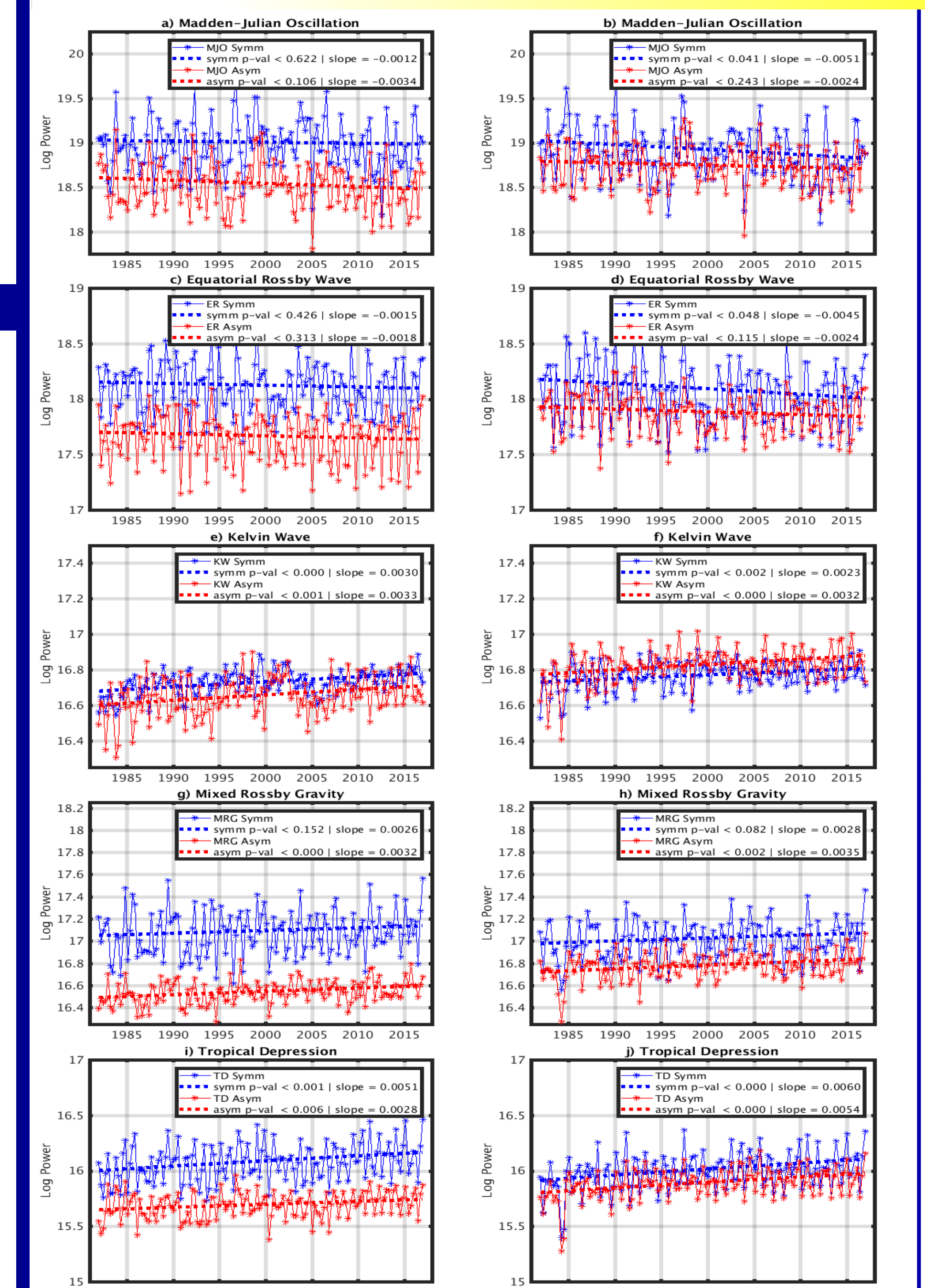


**Fig. 3:** Interannual variations in the regional (see Fig. 1 for domain) mean power (red for antisymmetric part, and blue for symmetric part). OLR (left column), and  $T_b$  (right column) datasets. The slope, and the  $p$ -value ( $p$ -val) of the linear trend lines are shown in the box embedded in each panel.

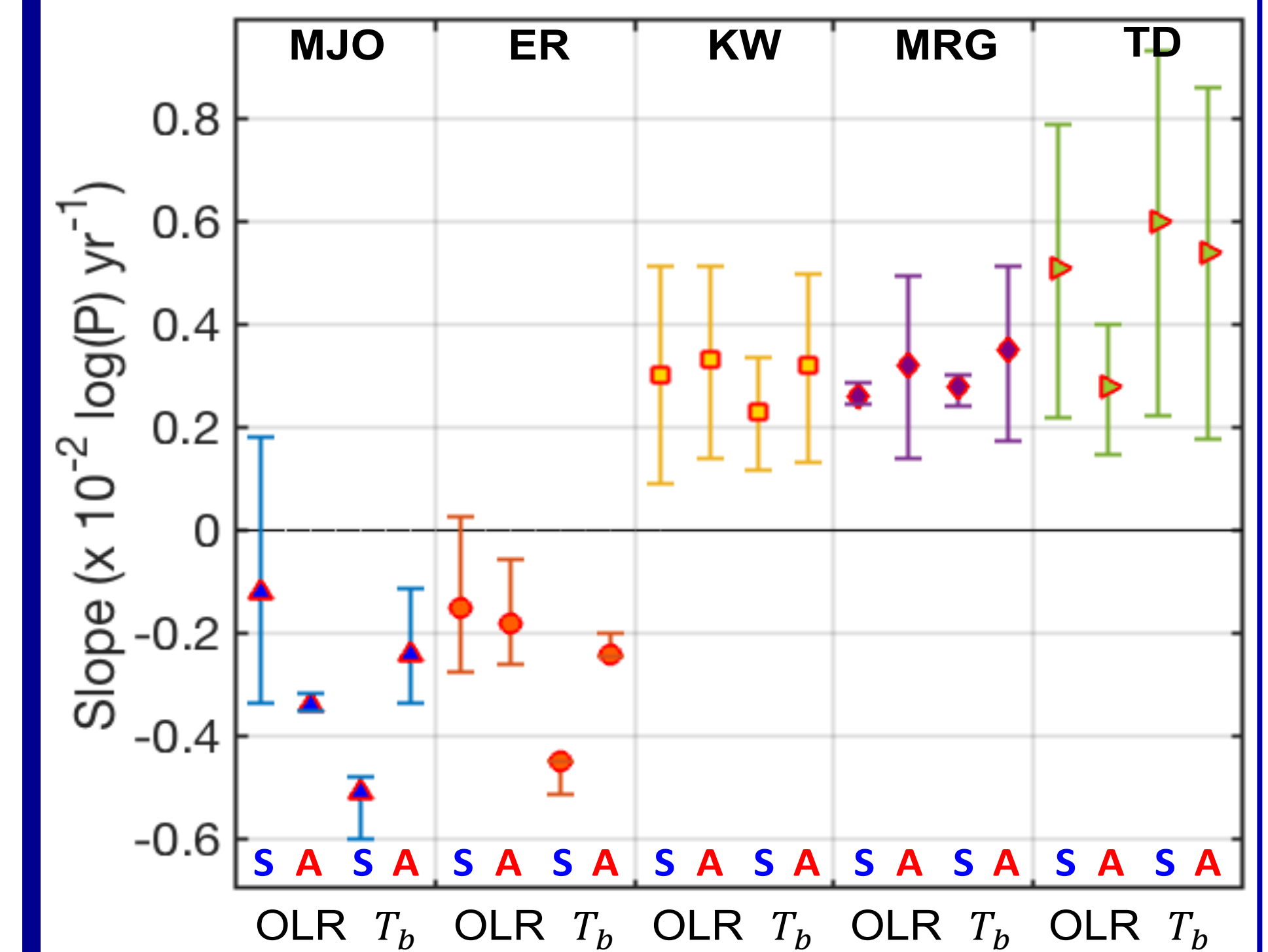


**Fig. 4:** A Monte Carlo analysis carried out by randomly rearranging the data points for each interannual variability curve 1,000 times in Fig. 3 without repetition in order to quantify uncertainties in the slope (units:  $\times 10^{-2} \log_e(P) \text{ year}^{-1}$ ) of the linear trend line shown in Fig. 3.

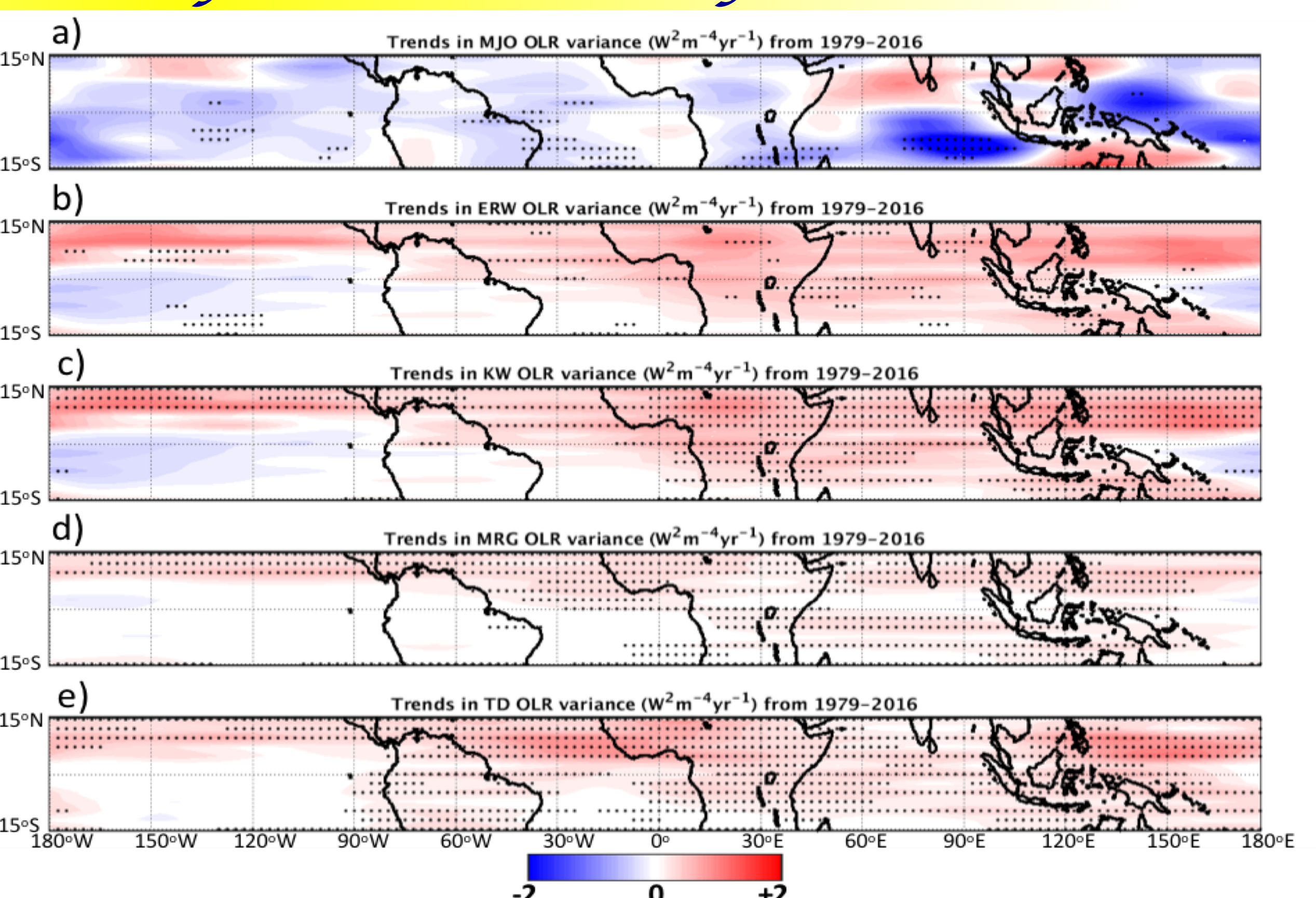


**Fig. 5:** Trends in OLR variance calculated using the spectrally filtered OLR anomaly for different wave types from 1979–2016. The black dots indicate trends that are statistically significant ( $p$ -value<0.1).

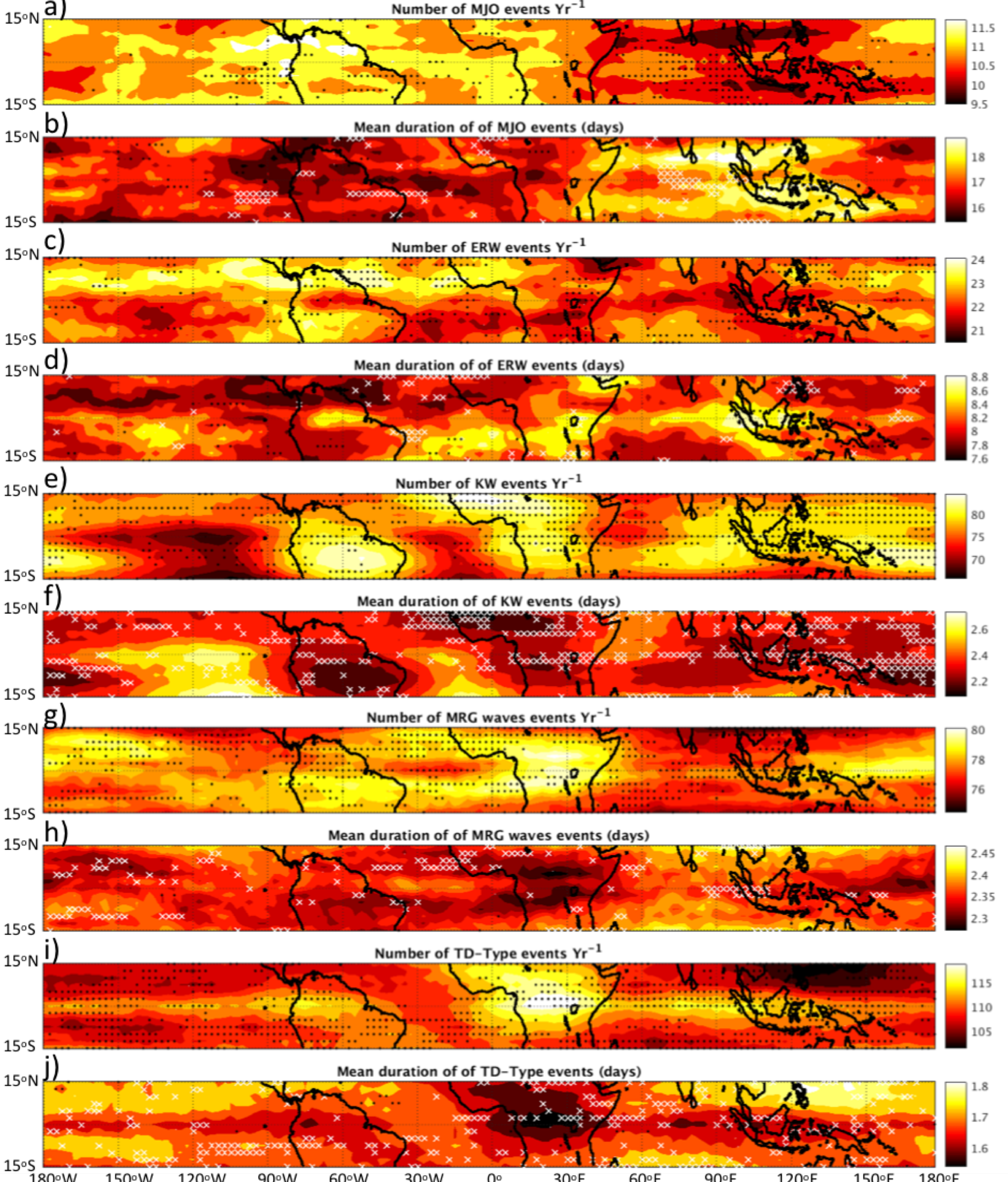


**Fig. 6:** The mean number, and duration of events corresponding to the different wave types from 1979–2016 using daily OLR anomalies. Significant ( $p$ <0.1) increasing (black dot) and decreasing (white cross) trends shown after applying a linear regression analysis ( $p$ -value<0.1).

## Future Work

- Diagnosing changes in the characteristics of tropical waves (e.g.,  $f$ , amplitude, and persistence), and identifying mechanisms resulting in the observed change in the  $P$  spectrum.
- Understanding the linkage between tropical waves and precipitation, and using projected changes in tropical wave activity to estimate precipitation change in possible future climate scenarios.
- El Niño–Southern Oscillation variability does not control the trends observed in the  $P$  spectrum (see extended abstract), but understanding the combination of ENSO and global warming on regional and global precipitation warrants further study.

Stay tuned for...

Raghavendra, A., P. E. Roundy, and L. Zhou, 2019: Trends in Tropical Wave Activity from the 1980s to 2016. *Journal of Climate*